2011, 21(33), 12280−12287.
37 Dakin, J. M.; Shanmugam, K. V. S.; Twigg, C.; Whitney, R. A.; Parent, J. S. Isobutylene-rich macromonomers: dynamics and yields of peroxide-initiated crosslinking. Polym. Chem. 2015, 53(1), 123−132.
38 Parent, J. S.; Porter, A. M. J.; Kleczek, M. R.; Whitney, R. A. Imidazolium bromide derivatives of poly(isobutylene-*co*-isoprene): a new class of elastomeric ionomers. Polymer 2011, 52(24), 5410−5418.
39 Kim, A.; Miller, K. M. Synthesis and thermal analysis of crosslinked imidazolium-containing polyester networks prepared by Michael addition polymerization. Polymer 2012, 53(25), 5666−5674.
40 Ye, Y. S.; Sharick, S.; Davis, E. M.; Winey, K. I.; Elabd, Y. A. High hydroxide conductivity in polymerized ionic liquid block copolymers. ACS Macro Lett. 2013, 2(7), 575−580.
41 Nykaza, J. R.; Ye, Y. S.; Elabd, Y. A. Polymerized ionic liquid diblock copolymers with long alkyl side-chain length. Polymer 2014, 55(16), 3360−3369.
42 Wu, J. R.; Huang, G. S.; Pan, Q. Y.; Zheng, J.; Zhu, Y. C.; Wang, B. An investigation on the molecular mobility through the glass transition of chlorinated butyl rubber. Polymer 2007, 48(26), 7653−7659.
43 Mora-Barrantes, I.; Malmierica, M. A.; Valentin, J. L.; Rodriguez, A.; Ibarra, L. Effect of covalent cross-links on the network structure of thermo-reversible ionic elastomers. Soft Matter 2012, 8(19), 5201−5213.
44 Marin, N.; Favis, B. D. Co-continuous morphology development in partially miscible PMMA/PC blends. Polymer 2002, 43(17), 4723−4731.
45 Harrats, C.; Thomas, S. and Groeninckx, G. "Micro- and nanostructured multiphase polymer blends system", CRC Press, 2006, p. 4-33.
46 Phetwarotai, W.; Tanrattanakul, V.; Phusunti, N. Synergistic effect of nucleation and compatibilization on the polylactide and poly(butylene adipate-*co*-terephthalate) blend films. Chinese J. Polym. Sci. 2016, 34(9), 1129−1140.
47 Nagarajan, V Overc.oming the fundamental challenges in improving the impact strength and crystallinity of PLA biocomposites: influence of nucleating agent and mold temperature. ACS Appl. Mater. Interfaces 2015, 7(21), 11203−11214.
48 Yu, F.; Huang, H. X. Simultaneously toughening and reinforcing poly(lactic acid)/thermoplastic polyurethane blend *via* enhancing interfacial adhesion by hydrophobic silica nanoparticles. Polym. Test. 2015, 45, 107−113.
49 Zhang, K. Y.; Mohanty, A. K.; Misra, M. Fully biodegradable and biorenewable ternary blends from polylactide, poly(3-hydroxybutyrate-*co*-hydroxyvalerate) and poly(butylene succinate) with balanced properties. ACS Appl. Mater. Interfaces 2012, 4(6), 3091−3101.
50 Zhang, K. Y.; Nagarajan, V.; Misra, M.; Mohanty, A. K. Super toughened renewable PLA reactive multiphase blends system: phase morphology and performance. ACS Appl. Mater. Interfaces 2014, 6(15), 12436−12448.

Reversible Protein Adsorption on PMOXA/PAA Based Coatings: Role of PAA

Yan-Mei Wang
Fujian Architecture School

Abstract In this study we report design of stimuli-responsive coating based on poly(2-methyl-2-oxazoline-random-glycidyl methacrylate) (PMOXA-*r*-GMA) comb copolymer and poly(acrylic acid)-block-poly(glycidyl methacrylate) (PAA-*b*-PGMA) block copolymers and scrutinize its ability to control protein adsorption. Firstly, PMOXA/PAA based coatings were prepared by simply spin coating the mixture of PMOXA-*r*-GMA and PAA-*b*-PGMA copolymer solutions onto silicon substrates followed by annealing at 110 °C. Then coatings were rigorously characterized by X-ray photoelectron spectroscopy (XPS), the static water contact angle (WCA) test, ellipsometry and atomic force microscopy (AFM). After that,the relationship of switchable behavior of PMOXA/PAA based coatings with PAA content and chain length was investigated through the change of thickness and WCA upon pH and ionic strength (*I*) trigger, which indicated that the change in thickness and WCA was triggered when PAA contents were increased as well as by increasing chain length of PAA in PMOXA/PAA based coatings. Finally, real-time adsorption/desorption of lysozyme (Lyso) on PMOXA/PAA based coatings was monitored using quartz crystal microbalance with dissipation monitoring (QCM-D). The results showed that the Lyso adsorption amount was increased upon increasing chain length and contents of PAA in PMOXA/PAA based coatings. The adsorbed Lyso was then efficiently desorbed by changing pH and *I* of medium with the maximum desorption (> 90% desorption percentage) observed for the suitable ratio of PMOXA and PAA while chain length of PAA was kept longer than that of PMOXA. Furthermore, the prepared coatings were found to repeatedly adsorb and desorb Lyso for four successive cycles of adsorption/desorption, which confirmed the stability of prepared coatings.

Keywords Binary polymer brushes; Stimuli-responsive coating; Reversible protein adsorption; Quartz crystal microbalance

INTRODUCTION

Precise control of protein adsorption/desorption on the surface is one of the most fundamental requirements in several fields, such as a biosensor, drug delivery, nanotransport tools, *etc*[1−8]. Reversible protein adsorption on the surface is thus desirable for these applications, which could be realized using interfaces modified with binary mixed polymer brushes. Such binary mixed brushes are normally composed of stimuli-responsive polymer chains and protein repellent polymer chains that are end-grafted to a substrate[9]. They could expose alternately one of the two components upon external stimuli (pH, ionic strength (*I*), temperature, *etc*.) and thus build stimuli-responsive (or smart) surfaces to control the protein adsorption/ desorption[10− 12].

For instance, Hoy *et al*. have performed a study of fibrinogen (FIB) (pI ~ 5.4) adsorption onto mixed brushes of poly(ethylene glycol) (PEG) and amphiphilic block copolymer poly(acrylic acid)-*b*-polystyrene (PAA-*b*-PS) at different pH and *I* values[12]. PEG brushes exhibited as protein repellent part due to its excellent hydrophilicity, and PAA block, an inherently responsive polyelectrolyte, served as a macromolecular actuator to bring the PS hydrophobic component (attached to the PAA tail) to the surface through significant variations in swelling of PAA chains as a function of pH and *I*. The variation of the hydrophobic-hydrophilic properties of the surface was used to control FIB adsorption. They observed that block copolymer PAA-*b*-PS alone did not display a significant switching of protein adsorption in the presence of $CaCl_2$, while the PAA-*b*-PS/PEG mixed brush demonstrated the complex synergic behavior of switching protein layer thickness from 0.3 nm to 4.0 nm at different calcium ion content levels. Delcroix *et al*. have designed poly(ethylene oxide) (PEO) and poly(acrylic acid) (PAA) mixed brushes and tuned their properties towards human serum albumin (HSA) adsorption by adjusting pH and *I* conditions[13, 14]. They concluded that in mixed PEO/PAA brushes, at pH 5 and low *I* ($I = 10^{-5}$ mol/L), PAA

chains were swollen in solution and mixed PEO/PAA brush could adsorb high quantity of HSA. At pH 9 and high I (I = 10^{-1} mol/L), PAA chains were shrunk and PEO chains were more exposed to the outermost surface, therefore, the adsorbed HSA could be desorbed with high efficiency from the mixed PEO/PAA brushes.

Later on, the same group has systematically investigated the reversible adsorption/desorption of HSA, lysozyme (Lyso), collagen (Col), and immunoglobulin G (IgG) on mixed PEO/PAA brushes, four very different proteins in terms of size, solubility, and isoelectric point[15]. The highest amount of Lyso adsorbed on the PEO/PAA brushes occurred at pH 7 and low ionic strength (I = 10^{-5} mol/L) and the maximum desorption for Lyso occurred at pH 3 and high ionic strength (I = 10^{-1} mol/L). The adsorption and desorption of Col andIgG on PEO/PAA binary brushes were also strongly dependent on swelling and collapsed conformations of PAA as well as protein repellency of PEO. They concluded that the amounts of protein adsorbed on mixed PEO/PAA brushes were of the same order of magnitude as on pure PAA brushes, while desorption efficiency was close to that of pure PEO, thus the mixed brushes nicely combined the properties of pure PAA and pure PEO brushes. Recently, Bratek-Skicki *et al.* tuned adsorption of HSA, FIB and Lyso on PEO/PAA mixed brushes considering the role of PEO amount in the brushes, regulated by changing its molar mass or its fraction in the solution used for polymer grafting[16]. They observed a decrease in the adsorbed amount of Lyso and FIB while increasing the PEO content and its molar mass in the mixed brushes, and under selected I and pH conditions, protein adsorption was mainly governed by the swelling/collapse behavior of PAA chains and by the contribution of electrostatic interactions.

Although many researchers have reported using PEG in binary polymer brushes as a protein-repellent polymer, PEG is known to undergo degradation by (auto)oxidation and form ethers and aldehydes, which hampers its long-term applications. To overcome the disadvantages associated with PEG, poly(2-oxazoline)s (POx), in particular, the water-soluble poly(2-methyl-2-oxazoline) (PMOXA), a peptidomimetic polymer, have lately drawn increasing attention for their excellent protein resistance[17–20]. Keeping in view PMOXA advantages, our group has synthesized PMOXA and PAA binary polymer brushes to control adsorption of bovine serum albumin (BSA). PMOXA/PAA mixed brushes were prepared by the sequential grafting of amine-terminated PMOXA (PMOXA-NH_2) and thiol-terminated PAA (PAA-SH) onto poly(dopamine) (PDA)-coated surfaces[21]. Mixed brushes with PAA chain length longer than PMOXA displayed better control toward protein adsorption/desorption behaviour and the maximum BSA desorption (about 87% desorption percentage at pH 9 and I = 10^{-1} mol/L) was observed when PAA chain length in the mixed brush was about 2.5 times that of PMOXA. To avoid multistep grafting process for PDA-coated surfaces, recently, we have prepared PMOXA/PAA based coatings by spin coating the solution of poly(2-methyl-2-oxazoline-random-glycidyl methacrylate) (PMOXA-*r*-GMA) comb copolymer and poly(acrylic acid)-block-poly(glycidyl methacrylate) (PAA-*b*-PGMA) block copolymer onto silicon/glass substrates following simple annealing protocol[22]. The surface composition of mixed brush could be controlled by simply adjusting mass percentages of both copolymers solution during spin coating and then the control of BSA adsorption/desorption upon pH and I change could be reached with this mixed brush modified surface.

In the present work, our purpose is to investigate the effect of PAA chain length and contents of PAA towards switchable adsorption/desorption behaviour of basic protein (Lyso). To do so, the PMOXA-*r*-GMA comb copolymer with fixed PMOXA chain length and PAA-*b*-PGMA block copolymer with different chain lengths of PAA block were synthesized *via* cationic ring-opening polymerization (CROP) of 2-methyl-2-oxazoline (MOXA) and reversible addition-fragmentation chain transfer (RAFT) polymerization of acrylic acid (AA) followed by their random and block copolymerization with glycidyl methacrylate (GMA), respectively. A wide range of PMOXA/PAA based coatings with the varied percentage of both copolymers were then grown on silicon/QCM-SiO_2 substrates using GMA anchoring segments *via* annealing process. We systematically investigated the stimuli-responsive properties of PMOXA/PAA mixed brushes with varying chain lengths and contents of PAA upon pH and I change. The influence of PAA chain length as well as PAA content on adsorption behaviour of Lyso was also investigated by means of quartz crystal microbalance with dissipation monitoring (QCM-D).

EXPERIMENTAL

Materials

The water used in all experiments was deionized water (LanLan Company, Hefei, China). 2-Methyl-2-oxazoline (MOXA, 99%, Sigma-Aldrich) was dried over calcium hydride for 24 h and distilled prior to use. Methyl trifluoromethansulfonate (MeOTf, ≥ 98%, Sigma-Aldrich) stored under nitrogen at 4 °C was used as received. 2,2′-Azobisisobutyronitrile (AIBN, Tianjin Guangfu Fine Chemical Research Institute, China) was recrystallized from ethanol and stored at 4 °C. Glycidyl methacrylate (GMA, 97%, Aladdin) was passed through an activated basic alumina column to remove the inhibitor before use. Acrylic acid (AA, Sinopharm Chemical Reagents, China) was distilled under reduced pressure and stored at 2 °C prior to use. Acetonitrile (ACN), dimethylformamide (DMF), triethylamine (TEA), methacrylic acid (MAA), *iso*-propanol (IPA), ethanol and other reagents were obtained from Sinopharm Chemical Reagents. ACN and TEA were dried over CaH_2 and distilled before use. IPA, DMF, and MAA were distilled under reduced pressure. *S*-1-dodecyl-*S*′-(*α*,*α*′-dimethyl-*α*″-acetic acid) trithiocarbonate (DDMAT) was synthesized according to the previously published procedure[23]. Lyso from hen egg white (M_w ~ 14.3 kDa, pI ~ 11.4, Biosharp Co., Ltd., Hefei, China) was purchased and used as received. HCl (Sinopharm Chemical Reagents), NaOH (Sinopharm Chemical Reagents) and NaCl (Sinopharm Chemical Reagents) were used to prepare saline

solutions of adjusted pH and *I* values. Silicon(111) wafers with a naturally oxidized layer were received from Zhejiang Crystal Photoelectric Technology Co. (Zhejiang, China). For QCM measurements, the crystals (QSX 303 SiO_2) used were thin AT-cut quartz coated with 50 nm of SiO_2, purchased from Biolin Scientific, Sweden.

Polymer Syntheses

Synthesis of PMOXA-r-GMA

PMOXA-*r*-GMA comb copolymer was synthesized according to our previous work[22]. Following the procedure, methacrylate terminated poly(2-methyl-2-oxazoline) (PMOXA-MA, DP = 23.5, contour chain length of PMOXA was 8.15 nm calculated by using Eq. S(1) (in electronic supplementary information, ESI), was synthesized by CROP of MOXA followed by its end-capping with MAA and TEA. Then, PMOXA-MA proceeded for random copolymerization with GMA using AIBN as an initiator to get PMOXA-*r*-GMA comb copolymer. Detailed synthesis procedure is shown in ESI. Feed molar ratio of PMOXA-MA to GMA was maintained at 3:1 in this work and relative number average molecular mass of PMOXA-MA and the molar ratio of PMOXA-MA to GMA was calculated by ^{1}H-NMR (Fig. S1 in ESI).

Synthesis of PAA-b-PGMA

The synthesis of PAA-*b*-PGMA di-block copolymer was performed by RAFT polymerization using PAA-macro RAFT agent. Initially, PAA-macroRAFT agent (DP = 27, 41 and 83, contour chain length of PAA was 6.78, 10.32, and 21.12 nm, respectively, calculated by using Eq. S2 of ESI) was synthesized according to previously reported procedure[24, 25]. Next, the di-block copolymer was prepared by adding calculated amounts of PAA-macroRAFT agent, GMA, DMF and AIBN into dried glass tube at 80 °C and reacting for 12 h under vacuum. The synthesized polymer was then purified by dialysis and freeze-drying to obtain yellow solid of PAA-*b*-PGMA as the end product[22]. The detailed synthesis process is given in ESI. Feed molar ratio of PAA-macroRAFT agent to GMA was 1:0.5. Molecular mass, exact molar ratio and polydispersity index (PDI) of the synthesized block copolymer were determined by ^{1}H-NMR and gel permeation chromatography (GPC) measurements. ^{1}H-NMR spectra and GPC traces for PAA and PAA-*b*-PGMA with different molecular weights of PAA are shown in Figs. S2, S3, S4,and S5 (in ESI).

General procedure for surface modification

Covalently crosslinked copolymer films of synthesized polymers were prepared by "grafting to" method *via* spin coating (KW-4A, Institute of Microelectronics of Chinese Academy of Sciences, Beijing, China), following the annealing protocol as reported by us in previous work[22, 26]. Prior to copolymer adsorption, the silicon wafers were cut into 1 cm × 1 cm pieces and cleaned by sonication in acetone and ethanol to remove organic contaminants (grease, *etc.*), soaked for 2 h in piranha solution (H_2SO_4:H_2O_2) (7:3 by volume) (caution: solution is highly oxidative and should be handled with great care), rinsed extensively with deionized water and then dried under N_2 before use. QCM sensors (AT-cut quartz with 50 nm layer of SiO_2 deposited on top of the gold electrode) were washed by dipping them in piranha solution for 5 min at most, deionized water for 10 min followed by drying with N_2. Solutions of copolymers with PMOXA-*r*-GMA/PAA-*b*-PGMA mass ratio of 100/0 (pure PMOXA-*r*-GMA), 0/100 (pure PAA-*b*-PGMA), 90/10, 50/50 and 20/80 were prepared by mixing stock solutions of PMOXA-*r*-GMA and PAA-*b*-PGMA at 10 mg/mL in deionized water at the given ratio in volume. Spin coating of copolymer solutions was performed on all these substrates for 60 s at 2000 r/min under vacuum. Prepared surfaces were named as $PMG_x/PAG_{y(n)}$, where 'PMG' and 'PAG' represent PMOXA-*r*-GMA and PAA-*b*-PGMA, '*x*' and '*y*' are the corresponding percentages of PMG and PAG in solution respectively and '*n*' is the DP of PAA. Corresponding prepared surfaces were named as PMG (pure PMOXA-*r*-GMA), PAG (pure PAA-*b*-PGMA), $PMG_{90}/PAG_{10(27)}$, $PMG_{50}/PAG_{50(27)}$, $PMG_{20}/PAG_{80(27)}$, $PMG_{90}/PAG_{10(41)}$, $PMG_{50}/PAG_{50(41)}$, $PMG_{20}/PAG_{80(41)}$, $PMG_{90}/PAG_{10(83)}$, $PMG_{50}/PAG_{50(83)}$, and $PMG_{20}/PAG_{80(83)}$, respectively. The coated substrates were subsequently annealed for 18 h at 110 °C. After annealing, substrates were allowed to cool to room temperature and washed with deionized water to remove unattached polymer and dried with N_2.

Characterizations

Nuclear magnetic resonance (NMR)

All ^{1}H-NMR spectra of polymers were recorded using an AVANCE 300 spectrometer (Bruker biospin, Switzerland) (300 MHz). The spectra were acquired at room temperature using deuterated chloroform ($CDCl_3$) or deuterium oxide (D_2O) as solvent and tetramethylsilane (TMS) was selected as an internal standard.

Gel permeation chromatography (GPC)

The molecular mass and polydispersity index (PDI = M_w/M_n) of PAA and PAA-*b*-PGMA polymers were determined by gel permeation chromatography (GPC, waters 1515) equipped with four ultrahydrogel columns and a refractive index detector (RI, Wyatt WREX-02). Phosphate buffer saline (pH 7.4) was used as eluent at a flow rate of 1.0 mL/min and the column oven temperature was kept at 35 °C. Molar masses were calculated against a conventional universal calibration with PEO as standard.

X-ray photoelectron spectrometer (XPS)

The XPS data were collected on a VG ESCALAB MK II X-ray photoelectron spectrometer (Thermo-VG Scientific Instruments, England) with an Al (Kα) X-ray source (1486.6 eV). All spectra were calibrated by setting the signal of the aliphatic (C, H) component of the C1s peak at 284.7 eV (rather than 285.0 eV, given the high proportion of aromatic carbon in the compounds). Surface composition (in case of mixed PMG/PAG brush) was calculated using peak areas measured after linear background subtraction and normalized on the basis of acquisition parameters, experimental sensitivity factors and transmission factors provided by the manufacturer[13, 22].

Variable angle spectroscopic ellipsometer (VASE)

The film thicknesses were measured by a spectroscopic ellipsometer (M-2000, Woollam Co., Inc., Lincoln, NE) at ~25 °C. The ellipsometric data were acquired in the spectral

range of 370–1000 nm at two different angles of incidence (65° and 75°). The analysis software, Complete EASE 4.81, was used to analyze all data. The reported thicknesses were the average of measurements made from at least three different spots on the polymer-modified wafer. To fit the ellipsometric data, the optical constants (refractive index, extinction coefficient) of Si (n = 3.865, k = 0.020) and SiO_2 (n = 1.465, k = 0) were used to determine the SiO_2 layer thickness of the freshly cleaned silicon surfaces. All the ellipsometric data were fit using Cauchy layer model to get the thickness of the brushes.

Atomic force microscopy (AFM)

The surface topology and surface roughness values of the unmodified and polymer modified silicon surfaces were evaluated on a DI MultimodeV atomic force microscope (AFM) from Veeco Instruments (Mannheim, Germany). The microscope was operated in tapping mode using Si cantilevers with a resonance frequency of 273 kHz and a drive amplitude of 1.30 V at a scan rate of 0.3 Hz. The AFM images were analyzed and post-processed using the NanoScope software (Version 5.12).

Switchable Properties

Hydrophilicity

The static water contact angles (WCA) were measured on an optical CA device (SL200KB, KINO Industry Co., Ltd, USA) equipped with CAST V2.28 software at ambient temperature using sessile drop method. A water drop with the volume of 1 µL was placed on the surface with a micro-syringe in an atmosphere of air and the values were recorded after 10 s. To check the switchable hydrophilic nature of brush surfaces, prepared surfaces were separately immersed in saline solutions of pH 5, 7, and 9 at $I = 10^{-5}$ mol/L and pH 3, 5, 7, and 9 at $I = 10^{-1}$ mol/L for 30 min respectively and WCA was measured for all pH values. Data presented were then averaged by three independent measurements on different locations of samples, and the results were reported as mean ± standard deviation.

Thickness

To evaluate pH-dependent thickness changes of polymer-modified silicon surfaces, the dry thickness of coated substrates was measured at different pH and ionic strength values. Firstly, polymer-modified substrates were separately immersed in pH 5, 7, and 9 at $I = 10^{-5}$ mol/L and pH 3, 5, 7, and 9 at $I = 10^{-1}$ mol/L solutions for 30 min each and then freeze-dried for 12 h. After that dry thickness of each substrate was measured at three different spots on polymer-modified wafer and the results were reported as a mean ± standard deviation. All the ellipsometric data were fit using Cauchy layer model to get the thickness of the brushes.

Protein adsorption test

The adsorption of Lyso was monitored *in situ* by QCM-D. Measurements were conducted using a Q-sense AB-system (Biolin Scientific, Sweden) at a temperature of (23.00 ± 0.1) °C. The crystal used was an AT-cut quartz crystal coated with a thin SiO_2 film (~50 nm, manufacturer specification), having a fundamental resonant frequency (f_0) of 5 MHz and a diameter of ~14 mm in a fluid cell with one side exposed to the solution. When the quartz QCM sensor is excited to oscillate in the thickness shear mode at its fundamental resonant frequency f_0, a small layer added to the electrodes induces a change in resonant frequency and dissipation energy (ΔD) of the sensor. In the present study, all the changes of Δf and ΔD were obtained from the measurements at the third overtone (n = 3), by bringing different solutions (Lyso and solvents) in contact with modified sensors. Sauerbery equation was then used to calculate layer mass (Δm):

$$\Delta m = -C\frac{\Delta f}{n} \quad (1)$$

where C is the mass sensitivity constant (C = 17.7 ng/(cm^2·Hz)) and n (= 1, 3…) is the overtone number[27]. Adsorption/desorption conditions for Lyso were chosen according to previously reported work[15]. For all QCM experiments, a baseline was recorded by flushing with deionized water for at least 10 min until constant Δf value was achieved. Then, the resonator was rinsed with a saline solution of adsorption (pH 7 and $I = 10^{-5}$ mol/L) to make protein adsorption surface for several minutes until the system reached equilibrium with constant Δf value. Freshly prepared Lyso solution (1 mg/mL in pH 7 and $I = 10^{-5}$ mol/L) was later introduced and decrease in frequency was noticed parallel to the adsorption of Lyso onto the polymer surface. After plateau reached for the frequency decrease, the resonator was again rinsed with the same saline solution for adsorption (with no protein) for 10 min. The saline solution of desorption (pH 3 and $I = 10^{-1}$ mol/L) was introduced in next step, followed by flushing with saline adsorption solution once again (without protein). At the end of the experiment, the resonator was rinsed with water to evaluate final desorption of protein. The same sequence of solutions was repeated for all experiments. To test the repeatability of adsorption/desorption process, the first adsorption/desorption cycle was repeated three to four times. At the end of the experiment, final rinsing was performed with deionized water. Baselines established between same solutions were used to determine changes in frequency shifts in order to avoid the effects of liquid phase on polymer brushes and the protein layer. The experiment was repeated three times with each resonator and average results for mass and frequency changes are presented here.

RESULTS AND DISCUSSION

Surface Modification

Silicon was chosen as model substrate for modification with PMG and PAG brushes. The surface composition of bare and modified substrate was determined by XPS analysis. Representative wide scan and C1s spectra of silicon before and after modification with polymer brushes are given in Fig. 1 and Figs. S6 and S7 (in ESI), respectively. Corresponding calculated element contents are summarized in Table1 and Table S1 (in ESI). Compared to the unmodified silicon surface, clear changes in carbon (C1s, 287 eV), nitrogen (N1s, 400.5 eV), oxygen (O1s, 533 eV), and silicon (154 eV for Si2s and 103 eV for Si2p) signals are observed in modified silicon surfaces. For PAG_{27}, PAG_{41}, and PAG_{83} (Fig. 1) coated silicon, effective suppression in

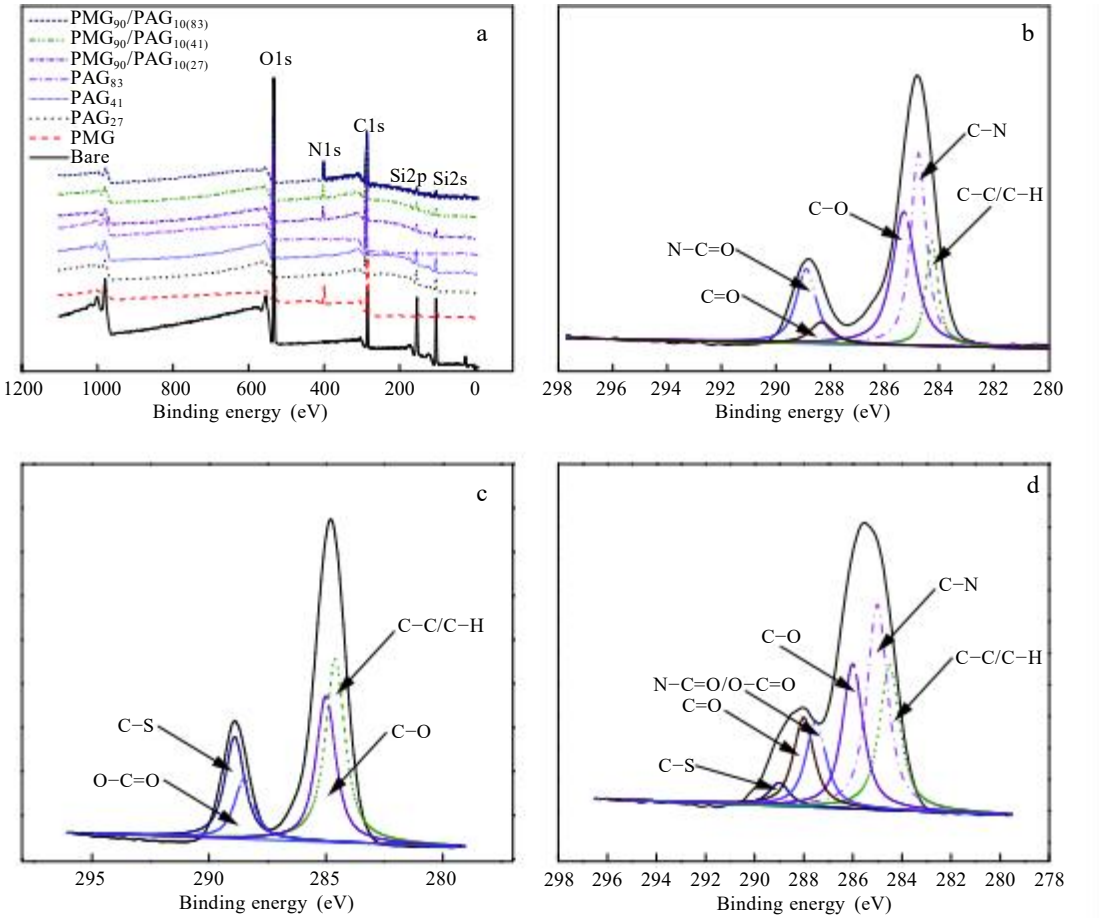

Fig. 1 (a) XPS wide scan spectra of bare, PMG, PAG_{27}, PAG_{41}, PAG_{83}, $PMG_{90}/PAG_{10(27)}$, $PMG_{90}/PAG_{10(41)}$, and $PMG_{90}/PAG_{10(83)}$ modified silicon surfaces, the high-resolution C1s of (b) PMG, (c) PAG_{83}, and (d) $PMG_{90}/PAG_{10(83)}$ modified silicon surfaces

Table 1 The atomic percentage of elements on the bare and polymer-modified silicon surfaces based on XPS, and corresponding dry thickness for modified surfaces

Sample	Element mole percent (atom %)						Thickness [a] (nm)
	C1s	O1s	N1s	Si2s	N/C	C/O	
Bare silicon wafer	23.47	46.53	0.32	29.38	0.01	0.5	_
PMG	60.33	20.07	9.09	4.11	0.15	3.0	3.48 ± 0.34
PAG_{27}	45.62	29.52	1.14	17.35	0.02	1.5	3.59 ± 0.91
PAG_{41}	54.81	31.95	1.03	15.28	0.02	1.7	4.76 ± 0.61
PAG_{83}	65.97	31.95	0.84	1.25	0.01	2.0	8.31 ± 2.46
$PMG_{90}/PAG_{10(27)}$	56.08	28.56	8.48	7.94	0.15	1.9	3.89 ± 0.16
$PMG_{90}/PAG_{10(41)}$	56.29	27.86	7.53	5.56	0.13	2.0	4.81 ± 0.19
$PMG_{90}/PAG_{10(83)}$	60.12	25.71	6.65	1.10	0.11	2.3	8.61 ± 2.68

[a] Obtained in dry film and expressed as mean ± SD (n =3)

substrate signals (154 eV for Si2s and 103 eV for Si2p) and increment in carbon (C1s, 287 eV) signal were observed. Also, in Fig. 1, a considerable increase in the N1s (400.5 eV) and C1s (287 eV) peaks respectively was observed for PMG-modified silicon wafer along with a corresponding decrease in Si2s and Si2p peaks. C/O ratio was also calculated for modified silicon substrates and it was observed that C/O ratio was increased from 0.5 to 3.0 when comparing bare and PMG-modified substrate respectively (Table 1). For PMG/PAG mixed brushes modified surfaces (1Fig. and Fig. S6 in ESI), disappearance of substrate Si signal (154 eV for Si2s and 103 eV for Si2p) and presence of C1s (287 eV), N1s (400.5 eV) and O1s (533 eV) confirmed the presence of both PMG and PAG copolymers on surface.

From Table 1, it can be observed that the ratio of nitrogen to carbon (N/C) was increased from 0.01 for bare to 0.15 for PMG-modified surface, favoring the presence of PMG on the surface. For PAG_{27}, PAG_{41}, and PAG_{83} modified surfaces, the ratio of N/C was found to be negligible *i.e.* 0.02, 0.02, and 0.01 respectively. A small amount of nitrogen may come from contaminations in the air or elsewhere. However, C/O ratio was increased from 1.5 to 1.7 and 2.0 for PAG_{27} to PAG_{41} and PAG_{83} modified substrates. Higher C/O ratio for PAG_{83} can be associated with a higher chain length of

PAG_{83} than PAG_{41} and PAG_{27}. For mixed brush modified surface, the corresponding ratio of N/C was 0.15, 0.13 and 0.11 for $PMG_{90}/PAG_{10(27)}$, $PMG_{90}/PAG_{10(41)}$, and $PMG_{90}/PAG_{10(83)}$ modified silicon surfaces, respectively. Their C/O ratio was also increased from 1.9 to 2.0 and 2.3,respectively. Results for other mixed brush compositions are given in Table S1 (in ESI). From Table 1 and Table S1 (in ESI), it can be seen that the Si2p signal characteristic of the bare silicon wafer was about 30%, which was decreased to 17.35%, 15.28% and 1.25% for PAG_{27}, PAG_{41}, and PAG_{83} and 4.1% for PMG-coated silicon surface. However, a dramatically decreased silicon signal was observed for all mixed PMG/PAG brush modified silicon substrates, pointing favor towards better surface coverage with a mixed brush than pure PMG and PAG. Moreover, the relative mass fraction of PMG and PAG (G_{PMG} and G_{PAG}) on the mixed brush modified silicon surface was also calculated from XPS data (the results are shown in Table S2 in ESI). When PMG/PAG mixed brush surfaces were fabricated by using the solution with the same mass composition (PMG_{90}/PAG_{10}, PMG_{50}/PAG_{50}, and PMG_{20}/PAG_{80}), the contour chain length of PAA (*i.e.* for PAG_{27}, contour chain length of PAA is 6.78 nm) was shorter than that of PMOXA (8.15 nm), surface was enriched with PMG contents more than PAG contents compared with the corresponding solution used for fabricating PMG/PAG mixed brush modified surface; when the contour chain length of PAA was slightly longer (*i.e.* for PAG_{41}, contour chain length of PAA is 10.32 nm), surface contained more PAG contents than PMG; when PAA length was about 2.6 times (*i.e.* for PAG_{83}, contour chain length of PAA is 21.12 nm) that of PMOXA, the surface was more enriched with PAG as compared to PMG. Higher PAG contents can be related to higher surfaces coverage for PAG when chain length of PAA is about 2.6 times that of PMOXA side chains.

The dry thickness of prepared coatings was estimated through VASE and data are presented in Table1 and Table S1 (in ESI). For PMG-coated surface, thickness of 3.48 nm was observed. For PAG-coated surfaces, the thickness was increased from 3.59 nm to 4.76 and 8.31 nm for PAG_{27} to PAG_{41}, and PAG_{83} coating. Higher thickness might be attributed to the longer contour chain length of PAA in PAG_{83} block copolymer than in PAG_{27} and PAG_{41} copolymers. Moreover, for PMG/PAG mixed brush modified surfaces of all composition, thickness value was slightly higher than those of PAG and PMG modified surfaces. Among all PMG/PAG mixed brush surfaces, a comparatively high thickness was observed for mixed brush containing PAG_{83} than PAG_{41} and PAG_{27}. The results are in line with the XPS data in which a strong reduction in Si signal for the PMG/PAG mixed brush modified surface was observed and the Si signal decreased more for corresponding mixed brush containing PAG_{83} (Table 1 and Table S1 in ESI).

These results are in accordance with the previous study of PEO/PAA mixed brush performed by Delcorix *et al.*, in which they found that PEO/PAA mixed brushes had better coverage for gold substrates than their homopolymer brushes (PAA or PEO) mainly due to a higher grafting density of the chains, giving a higher thickness layer[13]. Taking into account the thickness and XPS data, it is confirmed that silicon substrate could be modified successfully with PMG, PAG, and PMG/PAG mixed brushes with varied compositions and by increasing contour chain length of PAA *i.e.* from 6.78 nm to 21.12 nm, PAG contents became higher than PMG in PMG/PAG mixed brushes coatings.

To further characterize the grafting of polymer brushes on the silicon surface, the surface morphology was investigated by AFM with tapping-mode, and the corresponding 3D images are shown in Fig. 2 and Fig. S8 (in ESI). Root-mean-square roughness (Rq) for bare silicon surface (Fig. 2a) was changed from 0.31 nm to 0.55, 0.49, 0.46, 0.67, 0.71, 0.78, and 1.12 nm, upon subsequent grafting of PMG, PAG_{27}, PAG_{41}, PAG_{83}, $PMG_{90}/PAG_{10(27)}$, $PMG_{90}/PAG_{10(41)}$, $PMG_{90}/PAG_{10(83)}$ (Figs. 2b–2h). For $PMG_{50}/PAG_{50(27)}$, $PMG_{20}/PAG_{80(27)}$, $PMG_{50}/PAG_{50(41)}$, $PMG_{20}/PAG_{80(41)}$, $PMG_{50}/PAG_{50(83)}$, and $PMG_{20}/PAG_{80(83)}$ modified substrates, results are given in Fig. S8 (in ESI). It was noticed that the surface roughness was altered after coating with different compositions of PMG and PAG. Higher Rq values after grafting copolymer further reveal the successful modification of silicon surface by copolymer *via* thermal immobilization method.

The Switchable Behaviour of Brushes

The static water contact angle (WCA) measurement is the most convenient way to assess the hydrophilicity and wettability of solid surfaces, and the switchable hydrophilic properties indirectly determine the switchable antifouling properties of the surface. Fig. 3 summarizes the WCA values of PAG_{27}, PAG_{41}, PAG_{83}, $PMG_{90}/PAG_{10(27)}$, $PMG_{90}/PAG_{10(41)}$, and $PMG_{90}/PAG_{10(83)}$ modified silicon wafers at pH 5, 7, and 9 at $I = 10^{-5}$ mol/L and pH 3, 5, 7, and 9 at $I = 10^{-1}$ mol/L conditions. For $PMG_{50}/PAG_{50(27)}$, $PMG_{20}/PAG_{80(27)}$, $PMG_{50}/PAG_{50(41)}$, $PMG_{20}/PAG_{80(41)}$, $PMG_{50}/PAG_{50(83)}$, and $PMG_{20}/PAG_{80(83)}$, WCA results are shown in Fig. S9 (in ESI). Due to pH-independent nature of PMG, the variation of WCA of PMG was not significant in the range of investigated pH value and I (WCA value was (20° ± 5°) at all pH values)[22].

From Fig. 3(a), it can be seen that when I was fixed to 10^{-5} mol/L and pH value increased from 5 to 9, WCA decreased from 29° to 16° for PAG_{27}, 46° to 15° for PAG_{41}, and 65° to 16° for PAG_{83} modified surfaces; meanwhile, it can be seen that at pH 5 and 7, WCA of PAG-modified silicon wafer increased with the contour chain length of PAA, and the difference of WCA decreased with increasing pH value; when pH reached 9, WCAs were almost the same for all of PAG-modified surface whatever the contour chain length of PAA. Generally, at low I, while pH < pK_a (pK_a of PAA situated around 5), PAA chains are neutral and tend to shrink with a relatively hydrophobic behaviour; when the pH value approaches the pK_a, PAA chains in the uppermost layer begin to dissociate, although the majority of the brushes remain collapsed, and the ionized brush segments on the brush surface can stretch out into solution; the brush then swells with further increasing the pH value because of an

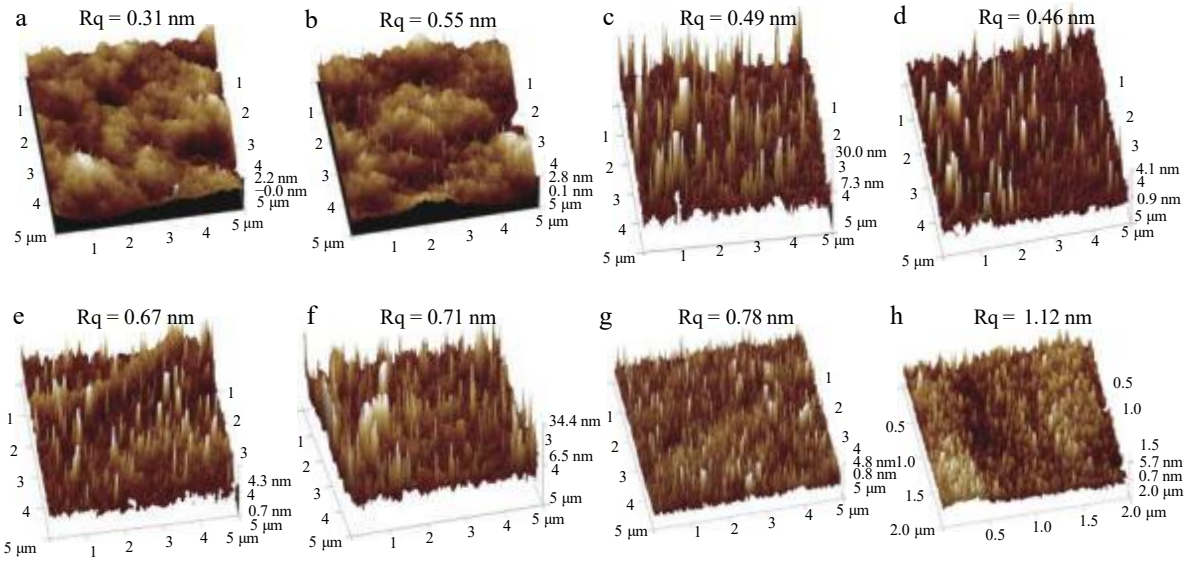

Fig. 2 AFM images of silicon wafers (a) before and (b–h) after PMG, PAG_{27}, PAG_{41}, PAG_{83}, $PMG_{90}/PAG_{10(27)}$, $PMG_{90}/PAG_{10(41)}$, and $PMG_{90}/PAG_{10(83)}$ modification. The scan size was 5 μm × 5 μm.

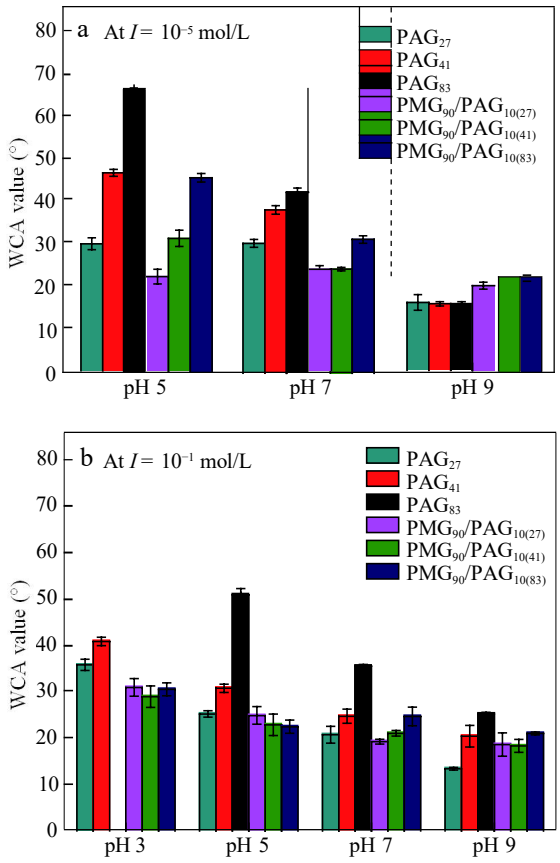

Fig. 3 WCA values of PAG_{27}, PAG_{41}, PAG_{83}, $PMG_{90}/PAG_{10(27)}$, $PMG_{90}/PAG_{10(41)}$, and $PMG_{90}/PAG_{10(83)}$ modified silicon wafers with varied pH values at (a) $I = 10^{-5}$ mol/L and (b) $I = 10^{-1}$ mol/L

increasing fraction of negative charges on PAA chains; when the pH value increases to 9, the density of negative charges on PAA chains increases largely, and the charged PAA chains stretch out as much as possible to reduce electrostatic repulsion between negative charges[28–30]. Considering the conformational changes of PAA mentioned above, higher WCA value at pH 5 and low *I* indicated relatively hydrophobic behaviour of PAG-modified silicon wafer, whereas at pH 7 and low *I*, WCA was decreased due to ionization of carboxylic groups along PAA chains, and extremely low WCA at pH 9 clearly indicated complete ionization of PAA chains and hydrophilic behaviour of PAG-modified silicon wafer at higher pH value. Higher WCA for PAG-modified silicon wafer with longer chain length at pH 5 and pH 7 at low *I* is related to the higher hydrophobicity of PAA as compared to that with shorter chains. At pH 9, the WCA was found almost the same (~16°) for all PAG-modified surfaces which is associated with complete dissociation of acid groups of PAA irrespective of the chain length of PAA. For $PMG_{90}/PAG_{10(41)}$ and $PMG_{90}/PAG_{10(83)}$ modified silicon wafer (*i.e.* the contour chain length of PAA is longer than that of PMOXA), when increasing pH value from 5 to 9 WCA decreased from 30° to 22° for $PMG_{90}/PAG_{10(41)}$ and from 45° to 21° for $PMG_{90}/PAG_{10(83)}$ modified surfaces, respectively; however, the change of WCA value was less than those of pure PAG_{41} and PAG_{83} modified surfaces. For $PMG_{90}/PAG_{10(27)}$ coating (*i.e.* the contour chain length of PAA is shorter than that of PMOXA), WCA value was not changed much from pH 5 to pH 9. The change in WCA values for other mixed brush surfaces is shown in Fig. S9(a) (in ESI). In mixed brush modified surfaces, when contour chain length of PAA (PAG_{41}, 10.32 nm; PAG_{83}, 21.12 nm) is longer than PMOXA side chains (8.15 nm), at pH 5 and low *I* PAA chains were partially negatively charged, swollen in solution, and partially exposed at the outermost surface, and the PAA chains then swelled with further increasing the pH value because of an increasing fraction of negative charges on PAA chains. It suggested that the properties of PMG/PAG mixed brushes were dominated by PAA chains during selected range of pH value at low *I* when the PAA chain length was longer than that of PMOXA chain, resulting in

the same trend of the WCA change with the pure PAG_{41} and PAG_{83} modified surfaces. When contour chain length of PAA (PAG_{27}, 6.78 nm) was shorter than PMOXA side chains in the mixed brush, PMOXA was exposed at the outermost surface during the investigated range of pH value; the properties of PMOXA became dominant in solution and WCA did not exhibit a significant change by changing pH values (Fig. 3a and Fig. S9a in ESI).

When I was high ($I = 10^{-1}$ mol/L) and pH value increased from 3 to 9, WCA decreased from 35° to 14° for PAG_{27}, 40° to 21° for PAG_{41} and 60° to 25° for PAG_{83} modified surfaces (Fig. 3b). In fact, at high I and the pH value below pK_a of PAA (*i.e.* at pH 3), PAA chains are neutral, display collapsed conformation and form intramolecular hydrogen bonds. When pH approaches pK_a of PAA *i.e.* at pH 5, PAA chains start to swell due to ionization of carboxylic groups. However, the extent of swelling is reduced due to the salt effect, which compensates for negative charges and causes shrinkage of chains. By further increasing the pH value to above pK_a (at pH 7 and 9), PAA chains are more collapsed, because at higher pH values and high I, the negative charges of PAA chains are screened by the electrostatic repulsions between solution counterions and ionized PAA chains[31, 32]. Theoretically, an increase in I is also shown to decrease the water-solid interfacial tension, which would have the effect of decreasing the contact angle. High I decreases the Debye screening length in solution so that at low pH values (below pK_a of PAA), PAA brush exhibits collapsed conformation and possesses hydrophobic behaviour to some extent[33, 34]. From conformational studies and theoretical approaches, herein, it can be seen that at pH 3, 5, and 7 values at $I = 10^{-1}$ mol/L, WCA for PAG_{27} was 35°, 25°, and 20°, for PAG_{41}, 40°, 30°, and 24°, and for PAG_{83}, 60°, 50°, and 35° respectively. However, the mixed brush surfaces *i.e.* $PMG_{90}/PAG_{10(27)}$, $PMG_{90}/PAG_{10(41)}$ and $PMG_{90}/PAG_{10(83)}$ modified surfaces displayed no significant change in WCA values (difference less than 5° between different pH values) at all pH values at high I value ($I = 10^{-1}$ mol/L), and the average WCA observed for PMG/PAG mixed brush surfaces was found to be near 25°, which is close to WCA observed for PMG-modified surfaces (about 23°). Similar results were observed for other mixed brush compositions (see Fig. S9b of ESI). These results further implied that at higher I conditions, PAA chains were collapsed and the PMOXA chains became more dominant in solution, resulting in WCA value of PMG/PAG mixed brush surface close to the WCA of PMG-modified surface.

The direct effect of the response of pH and I on the dry thickness of PAG and PMG/PAG mixed brush coatings was also investigated with varying chain lengths of PAA and results are shown in Fig. 4. As can be seen from Fig. 4(a), at low ionic strength ($I = 10^{-5}$ mol/L), the thickness of PAG-modified surfaces was increased with increasing the pH value from 5 to 9 whatever the PAA chain length was, and a more obvious increase in thickness by increasing the pH value was noticed for the longer PAG brushes modified silicon wafer *i.e.* PAG_{41} and PAG_{83} as compared to PAG_{27}. The higher thickness value is linked to increasing

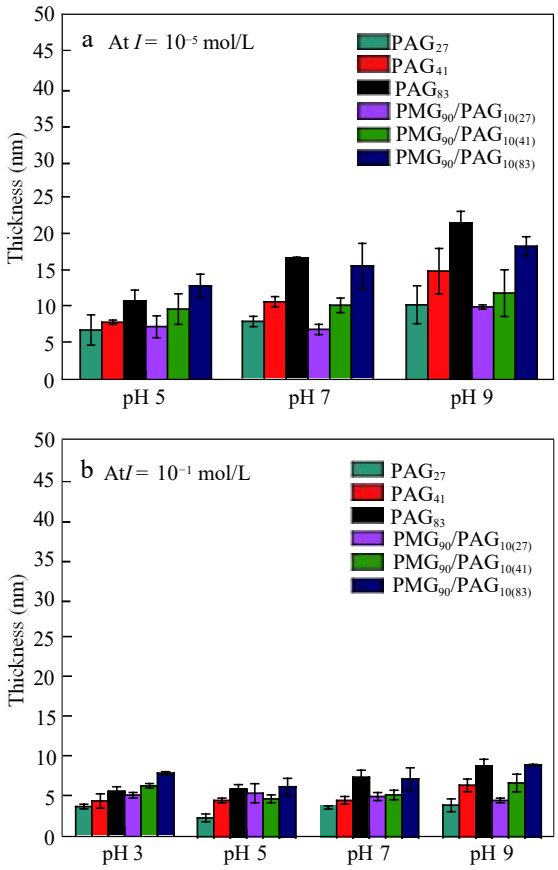

Fig. 4 The thickness of PAG_{27}, PAG_{41}, PAG_{83}, $PMG_{90}/PAG_{10(27)}$, $PMG_{90}/PAG_{10(41)}$, and $PMG_{90}/PAG_{10(83)}$ modified silicon wafers with varied pH values at (a) $I = 10^{-5}$ mol/L and (b) $I = 10^{-1}$ mol/L

dissociation of carboxylic groups and the charged PAA chains stretching out as much as possible to reduce electrostatic repulsion which resulted in a higher thickness of PAG brush coated surfaces. PAA with the longer chain length contained more charged groups and formed a thicker layer at higher pH values. This finding is in line with previous research showing that longer PAA brushes (with chain length 22, 30 and 40 nm) exhibited more significant increase in thickness value when pH was increased from 3 to 10[30]. The same trend was observed for mixed brush *i.e.* 7 nm to 10 nm for $PMG_{90}/PAG_{10(27)}$, 9.5 nm to 12 nm for $PMG_{90}/PAG_{10(41)}$, and 13 nm to 18 nm for $PMG_{90}/PAG_{10(83)}$ modified surfaces. The increase of thickness upon increasing pH value is clearly an indication of increasing hydrophilicity of the surfaces as obviously demonstrated by WCA results, and the increased thickness value by increasing chain length of PAA is an explanation of dominant responsive properties of PAA in PMOXA/PAG mixed brush surfaces containing PAA chains longer enough than PMOXA chains.

When I was high ($I = 10^{-1}$ mol/L) and pH value increased from 3 to 9 (Fig. 4b), surface thickness was slightly increased from 3.6 nm to 4 nm for PAG_{27}, 4.3 nm to 6.6 nm for PAG_{41}, and 5.5 nm to 9 nm for PAG_{83} modified surface respectively and the increase in thickness was higher for longer PAA chains. The slight increase in the thickness with increasing pH value at higher I value is mainly due to the

screening effect which causes shrinkage of PAA chains and thus lowers the thickness[14]. For mixed brush surfaces, $PMG_{90}/PAG_{10(27)}$ surface did not display the significant difference of thickness between pH 3 and pH 9, but $PMG_{90}/PAG_{10(41)}$ and $PMG_{90}/PAG_{10(83)}$ modified surfaces displayed a difference of almost 2 nm between pH 3 and pH 9 values.

These results suggested that the thickness of both PAG and PMG/PAG mixed brush modified surfaces responded well to pH and *I* of the medium. At low *I*, the thickness increased significantly by increasing pH value due to PAA swelling. Thickness was also increased by increasing pH at high *I*, however, the increment was small as PAA chains collapsed at high salt contents. Meantime, chain length of PAA was proved to have great effect on thickness of brushes. For example, in PMG/PAG mixed brushes, when the chain length of PAA was shorter than that of PMOXA, pH-responsive behavior was suppressed but PAA chains longer than PMOXA chains exhibited significant variation in thickness value upon pH and *I* trigger. When the chain length of PAA was about 2.6 times that of PMOXA, the change of thickness became more prominent, therefore, implying better switchable properties of longer PAA chains in PMOXA/PAA mixed brush coatings.

Results of WCA and thickness under different pH and *I* values revealed that PMG/PAG mixed brush possessed properties of both PMG and PAG. These results also suggested that the thickness and wettability of PMG/PAG mixed brush modified surfaces could be adjusted by pH and *I* change, which meant the PMG/PAG mixed brush modified surface might possess the switchable protein adsorption ability upon pH and *I* trigger.

Regarding basic protein Lyso (with pI ~ 11.4), it is positively charged at pH below its pI and negatively charged at pH above its pI. Delcroix *et al.* stated that Lyso adsorption on PEO/PAA mixed brush modified surfaces reached the maximum at pH 7 and $I = 10^{-5}$ mol/L conditions due to electrostatic attractions between positively charged Lyso and negatively charged PAA chains and desorption took place at pH 3 and $I = 10^{-1}$ mol/L conditions at which electrostatic interactions between collapsed PAA chains and Lyso were minimized[15]. Herein, the lower WCA value and higher thickness of PAG or PMG/PAG mixed brush at pH 7 and $I = 10^{-5}$ mol/L explained the ionized and swollen state of PAA chains. Lyso was positively charged at pH 7, so the electrostatic attractions between negatively charged PAA chains and positively charged Lyso could reinforce the natural ability of the swollen PAA to adsorbLyso. However, at high *I* (10^{-1} mol/L) and low pH value *i.e.* at pH 3, as PAA still possessed hydrophobic nature (higher WCA for PAG or PMG/PAG mixed brush modified surface) due to shrinking of PAA chains at high *I* and pH 3 (lower thickness for PAG or PMG/PAG mixed brush modified surface) and formation of intramolecular hydrogen bonding between PAA chains, electrostatic interactions were reduced between PAA and Lyso and thus the desorption of Lyso could take place. Considering previous work and the results of WCA and VASE obtained in this work, the adsorption and desorption conditions selected for Lyso were pH 7 and $I = 10^{-5}$ mol/L and pH 3 and $I = 10^{-1}$ mol/L respectively and the extent of adsorption/desorption was then quantitatively evaluated by QCM-D.

Protein Adsorption Studies

Fig. 5 presents typical QCM graphs for Lyso adsorption/desorption on bare, PMG, PAG_{27}, PAG_{41}, PAG_{83}, $PMG_{90}/PAG_{10(27)}$, $PMG_{90}/PAG_{10(41)}$, and $PMG_{90}/PAG_{10(83)}$ coated QCM-SiO_2 sensors, respectively. These figures display normalized Δf values for the third overtone and the corresponding ΔD values are given in Fig. S10 (in ESI). Additionally,QCM graphs for Lyso adsorption/desorption on $PMG_{50}/PAG_{50(27)}$, $PMG_{20}/PAG_{80(27)}$, $PMG_{50}/PAG_{50(41)}$, $PMG_{20}/PAG_{80(41)}$, $PMG_{50}/PAG_{50(83)}$, and $PMG_{20}/PAG_{80(83)}$ coated sensors are given in Figs. S11 and S12 (in ESI). As shown in Fig. 5, water was flowed in the first step to obtain baseline, then the saline solution of adsorption (pH 7 and $I = 10^{-5}$ mol/L), and then the protein solution (1 mg/mL Lyso in pH 7 and $I = 10^{-5}$ mol/L) were flowed for the protein adsorption process followed by saline solution of adsorption again to evaluate adsorption of protein. After that saline solution of desorption (pH 3 and $I = 10^{-1}$ mol/L) was flowed to trigger the protein desorption. Then again the saline solution of adsorption was flowed so that desorption could be measured by the same solutions. In the end, final rinsing was performed with water. As mentioned in experimental section, the experiment was repeated three times with each modified sensor (one graph from each sensor is presented here), and the average results of Lyso adsorbed amount ($\Delta m_{adsorption}$), amount remained on the sensor surface after desorption ($\Delta m_{after\ desorption}$) and desorption percentage (%) are summarized in Table 2.

From Table 2, it can be seen that bare QCM-sensor adsorbed 806 ng/cm^2 of Lyso at adsorption conditions, and a very small amount of adsorbed Lyso was removed at desorption conditions (15% desorption percentage). The adsorption amounts of Lyso on pure PMG brush modified sensor were very limited, and 97% of adsorbed Lyso was released after desorption steps (Table 2), implying that the surfaces modified with these brushes were highly protein-repellent as expected[35, 36]. PAG-modified surfaces could adsorb a large amount of Lyso at pH 7 and $I = 10^{-5}$ mol/L conditions whatever the contour chain length of PAA was. Adsorption amount also increased with increasing chain length of PAA. During desorption steps, partial desorption of Lyso occurred and desorption percentage was 24%, 35%, and 45% for PAG_{27}, PAG_{41}, and PAG_{83} modified sensors. Lyso, a positively charged protein molecule, at neutral pH and low *I* values would be surrounded by negatively charged counterions in the solution. When it was transferred into a PAA brush, it could act as a multivalent counterion for the PAA chains. As a result, monovalent counterions of the PAA chains (as PAA is negatively charged and in swollen state at neutral pH and low *I* conditions) and the protein molecules were released into the solution. This "counterion evaporation" increased the entropy of the system, so the electrostatic interactions between negatively charged PAA

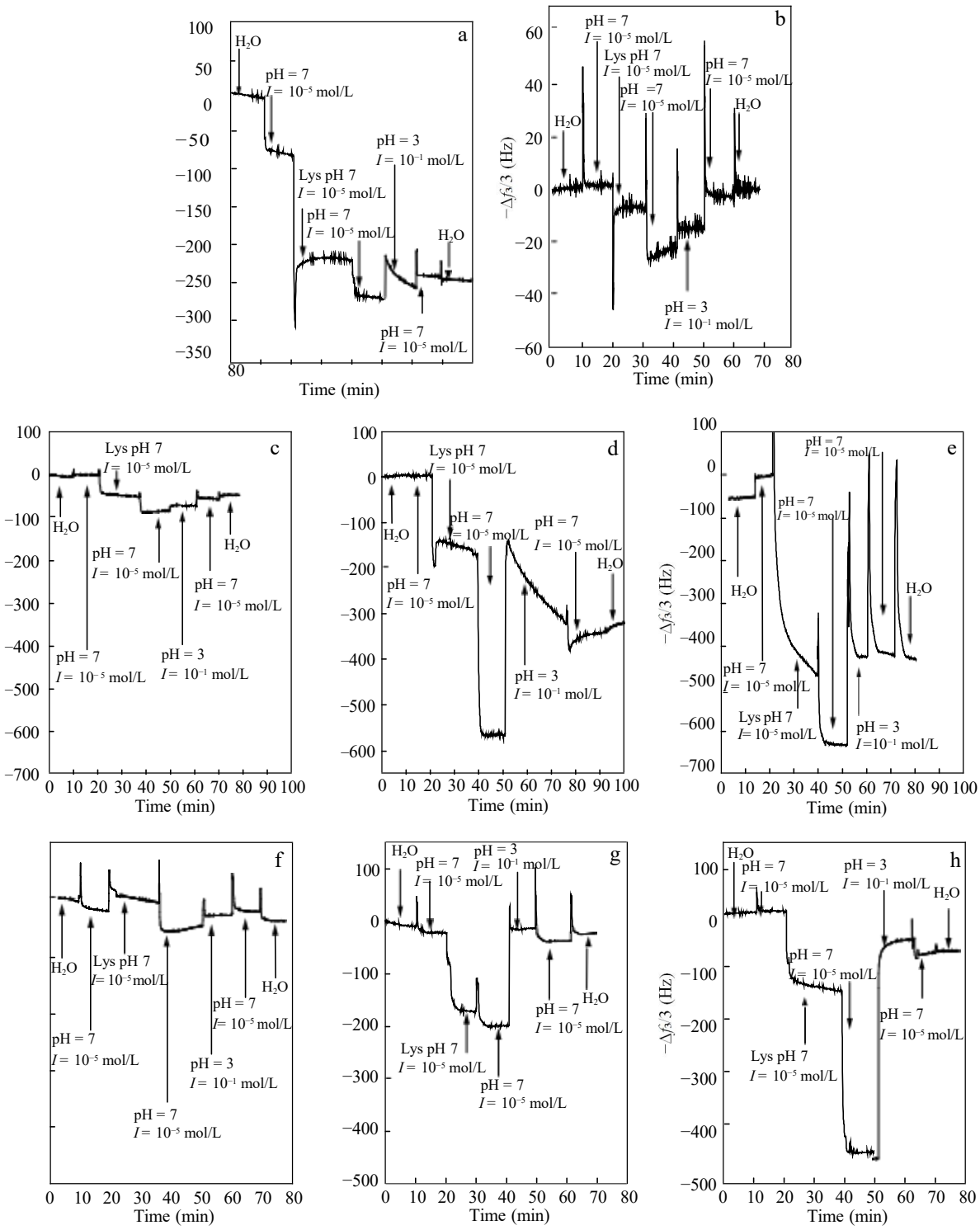

Fig. 5 Typical QCM graphs showing Δ*f* shifts after Lyso adsorption/desorption on (a) bare, (b) PMG, (c) PAG_{27}, (d) PAG_{41}, (e) PAG_{83}, (f) $PMG_{90}/PAG_{10(27)}$, (g) $PMG_{90}/PAG_{10(41)}$, and (h) $PMG_{90}/PAG_{10(83)}$ coated QCM sensor

chains and positively charged Lyso enabled a large amount of Lyso to beadsorbed on the surface until the ionic strength was the same inside and outside the PAA brush, when this counterion release was no longer related to an entropy increase[15]. However, at pH 3 and $I = 10^{-1}$ mol/L, PAA chains were hydrophobic and collapsed as seen from thickness and WCA results; Lyso was positively charged, but the collapsed conformations of PAA minimized the electrostatic interactions between both of them and thus desorption from surface took place[37, 38]. Higher adsorption experienced by the longer chain length of PAA was due to the higher specific surface developed by swollen PAA brushes of longer chain length compared to shorter ones, as noticed for higher WCA and thickness at pH 7 and *I* =

Table 2 Hydrated mass/unit area computed from QCM-D data using Sauerbrey equation after Lyso adsorption/desorption at (pH 7 and $I = 10^{-5}$ mol/L) and (pH 3 and $I = 10^{-1}$ mol/L), as well as resultant possible desorption percentage

Sample	$\Delta m_{adsorption}$ (ng/cm^2)	$\Delta m_{after\ desorption}$ (ng/cm^2)	Desorption percentage [a] (%)
Bare	806	688	15
PMG	210	7	97
PAG_{27}	1964	1486	24
PAG_{41}	2517	1574	35
PAG_{83}	3786	2104	45
$PMG_{90}/PAG_{10(27)}$	306	100	67
$PMG_{90}/PAG_{10(41)}$	1010	108	90
$PMG_{90}/PAG_{10(83)}$	1500	149	91
$PMG_{50}/PAG_{50(27)}$	1032	472	54
$PMG_{50}/PAG_{50(41)}$	1563	442	71
$PMG_{50}/PAG_{50(83)}$	3186	1121	64
$PMG_{20}/PAG_{80(27)}$	1121	649	42
$PMG_{20}/PAG_{80(41)}$	1616	778	51
$PMG_{20}/PAG_{80(83)}$	3540	1520	57

[a] Desorption percentage is calculated by using formula *i.e.* Desorption percentage (%)= $\frac{\Delta m_{adsorption} - \Delta m_{after\ desorption}}{\Delta m_{adsorption}} \times 100$

10^{-5} mol/L for longer PAG_{41} and PAG_{83} brushes compared to PAG_{27}. Higher desorption percentage for longer PAA brushes supported the strong protein repellent ability of longer brushes.

Regarding Lyso adsorption on PMG/PAG mixed brushes, two aspects were considered to examine adsorption behaviour. Firstly, it was noticed that adsorption amount of Lyso was increased on PMG/PAG mixed brushes by increasing PAG contents while the PAA chain length was fixed, meanwhile the desorption percentage was decreased with the increase of PAA contents on corresponding modified surfaces (see Table 2). For instance, adsorbed amount of Lyso on PMG_{90}/PAG_{10}, PMG_{50}/PAG_{50}, and PMG_{20}/PAG_{80} brushes with PAG_{27} was increased to 306, 784, and 1079 ng/cm^2, respectively. For PAG_{41}-modified surface, adsorption masses were 1010, 1563, 1616 ng/cm^2 for PMG_{90}/PAG_{10}, PMG_{50}/PAG_{50}, and PMG_{20}/PAG_{80} coating compositions, and for PAG_{83}-modified surfaces, adsorption masses were 1500, 3186, and 3540 ng/cm^2 for PMG_{90}/PAG_{10}, PMG_{50}/PAG_{50}, and PMG_{20}/PAG_{80} coating compositions, respectively. Desorption percentage for PMG_{90}/PAG_{10}, PMG_{50}/PAG_{50}, and PMG_{20}/PAG_{80} compositions was decreased from 67% to 54% and 42% for PAG_{27}, from 90% to 71% and 51% for PAG_{41}, and from 91% to 64%, and 57% for PAG_{83} modified sensors respectively. Secondly, the amount of Lyso adsorption increased with the increasing chain length of PAA on PMG/PAG brush modified sensor while the mass composition of PMG and PAG used for coating preparation was fixed (see Table 2 and Fig. S11 in ESI for respective frequency shifts). For example, upon a comparison of Lyso adsorption on PMG_{90}/PAG_{10} composition with PAG_{27}, PAG_{41}, and PAG_{83} brushes, the amount of Lyso adsorption was increased to 306, 1010, and 1500 ng/cm^2, respectively.

To compare the effect of chain length of PAA and PMOXA, it is observed that when PAA chains were shorter (6.78 nm) than PMOXA side chains (8.15 nm), the adsorption and desorption amount of Lyso on PMG/PAG mixed brush modified sensors was less than that on PMG/PAG mixed brush with PAA chains longer (10.32 and 21.12 nm) than PMOXA chains. It can be stated that when the chain length of PAA was shorter (PAG_{27}, 6.78 nm) than PMOXA in PMG/PAG mixed brush, at pH 7 and low I (10^{-5} mol/L) values, although PAA chains were ionized and swollen, they could not be well exposed to surface due to the effect of longer chain length of PMOXA side chain, resulting in less adsorption mass of Lyso. When the PAA chains (PAG_{41}, 10.32 nm) were little longer than PMOXA chains (8.15 nm) in the PMG/PAG mixed brush, at pH 7 and lower I, PAA chains were negatively charged, swollen in solution, and more exposed at the outermost surface than PMOXA chains, enabling a large amount of Lyso in the solution to contact with exposed PAA chains easily, and hence the brush could adsorb a higher quantity of Lyso. Upon further increasing PAA chain length (PAG_{83}, 21.12 nm) almost 2.6 times that of PMOXA chains, PAA chains were more exposed in solution as compared to PAG_{41}-based mixed brushes, which further increased the adsorption amount of Lyso. Upon raising I to 10^{-1} mol/L at pH 3, PAA chains collapsed with hydrophobic nature, thereby the contact between Lyso and PAA decreased due to the minimization of electrostatic attraction between PAA (not charged) and Lyso (positively charged); at the same time, PMOXA chains were more exposed in the solution so the Lyso molecules came into contact with PMOXA chains, which then repelled them, and therefore Lyso was efficiently released from surface. That is why desorption percentage for mixed brush was higher than pure PAG brush as verified by QCM results of Lyso. The results above suggested that PMG/PAG mixed brush modified surface with controlled PMG and PAG composition was successfully achieved and protein adsorption/desorption could also be effectively controlled under pH and I stimuli by simply maintaining PMG/PAG percentage in solution while preparing the coatings as well as by PAA chain length in designing surface properties.

To further check the stability of PMG/PAG mixed brush system, $PMG_{90}/PAG_{10(41)}$ and $PMG_{90}/PAG_{10(83)}$ mixed brush modified sensors were selected to test the repeatability of

switchable adsorption/desorption behaviour due to their higher desorption percentage (~90%). Typical QCM graphs for the 3rd overtone are shown in Figs. 6(a) and 6(b), and calculated Δf shifts are given in Fig. 6(c). Real-time QCM graphs for corresponding modified QCM-sensors are shown in Figs. S13 and S14 (in ESI). For $PMG_{90}/PAG_{10(41)}$, observed Δfvalues were 125, 135, 115, and 125 Hz for four adsorption cycles. The same surface also displayed good desorption efficiency with observed Δfvalues of 0, 10, 20, and 20 Hz during desorption cycles. As mentioned above for longer chain length of PAA (PAG_{83}), during reversible adsorption/desorption of Lyso, $PMG_{90}/PAG_{10(83)}$ also displayed higher Δf values *i.e.* 180, 170, and 170 Hz for three repeating cycles of adsorption, representing the higher amount of adsorbed protein; besides, the desorption percentage was almost the same (more than 85%) for $PMG_{90}/PAG_{10(41)}$ and $PMG_{90}/PAG_{10(83)}$ coatings.

From above discussion, it is clear that PMG/PAG mixed brush coatings nicely combined properties of both PMOXA (protein repellent properties) and PAA (protein adsorbing properties), and respective Lyso adsorption/desorption properties were quite reversible and could be adjusted simply by maintaining percentage of both copolymers in solution, by maintaining chain length of PAA block and by tuning pH and *I*of the medium.

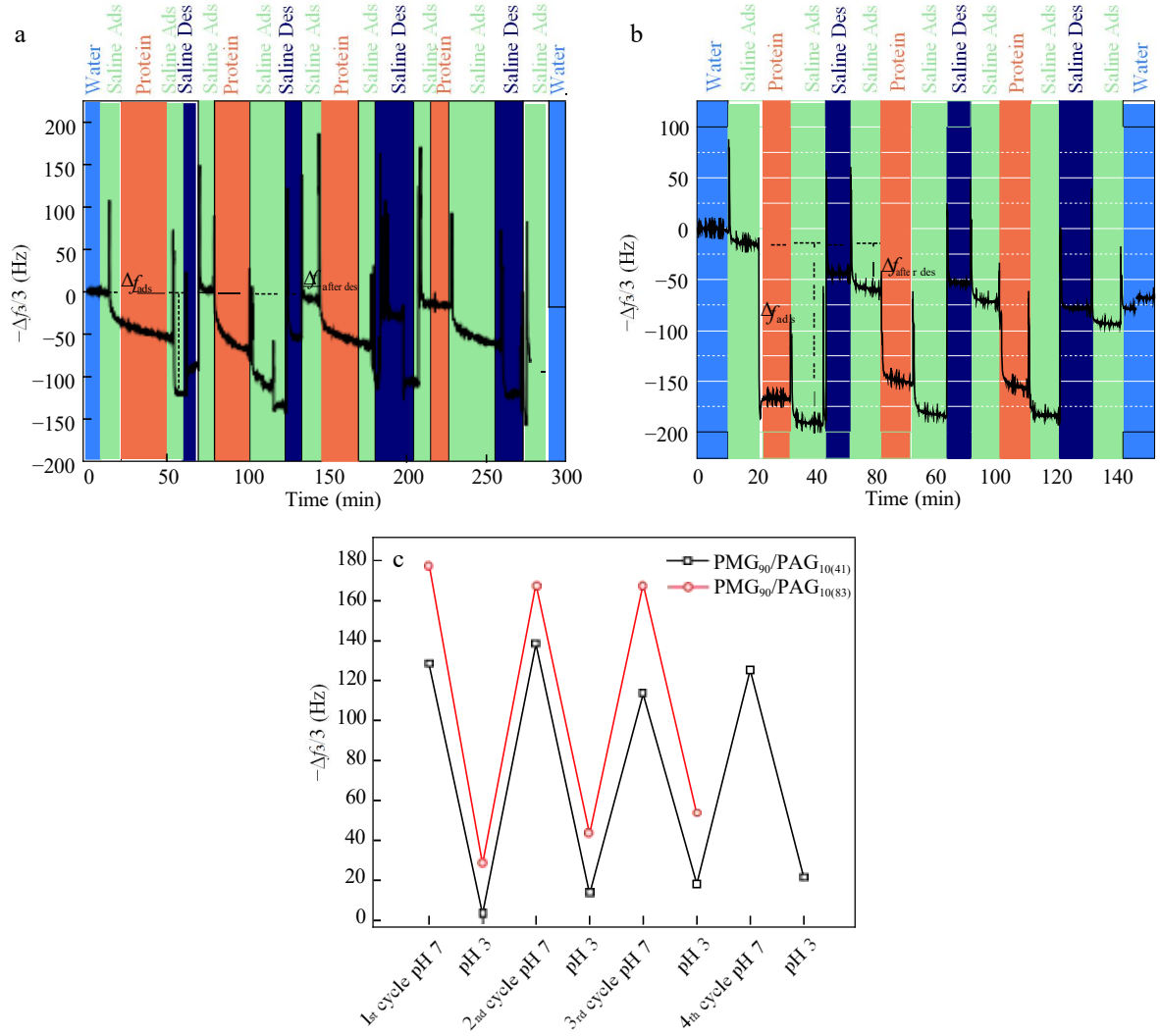

Fig. 6 QCM graph showing Lyso adsorption/desorption cycles on (a) $PMG_{90}/PAG_{10(41)}$, (b) $PMG_{90}/PAG_{10(83)}$ coated sensors (highlighted areas indicate different solution changes) and (c) calculated values of Δf shifts for three to four successive cycles of Lyso adsorption/desorption cycles

CONCLUSIONS

In this study, PMOXA/PAA based mixed coatings with a varied ratio of PMOXA and PAA and different chain lengths of PAA were prepared by simply spin coating the mixed solution of PMOXA-*r*-GMA comb copolymer and PAA-*b*-PGMA block copolymer with the desired percentage followed by annealing procedure. The role of PAA in mixed brushes, regulated by changing its contents and its chain length, was elucidated. Prepared coatings displayed pH and *I* dependent switchable hydrophilicity and thickness. Among

mixed brush coatings, the higher change in hydrophilicity and thickness was noticed for mixed brushes containing longer PAA chains and higher contents of PAA at selected pH and *I* conditions. The study of adsorption/desorption of Lyso on modified surfaces indicated that in PMOXA/PAA mixed brush surfaces, when PAA chain length was kept constant and contents of PAA were increased, the adsorption amount of Lyso increased under the selected pH and *I* conditions. Similarly, when PAA contents were fixed, it was observed that adsorption amount increased by increasing chain length of PAA and the maximum adsorption was noticed for $PMOXA_{90}/PAA_{10(83)}$ mixed brush surface having PAA chains 2.6 times that of PMOXA side chains. The adsorbed protein was efficiently removed (91% desorption percentage) from PMOXA/PAA based coating with $PMG_{90}/PAG_{10(41)}$ and $PMG_{90}/PAG_{10(83)}$ compositions where the chain length of PAA was longer than that of PMOXA. Furthermore, respective coatings displayed repeatable behaviour towards Lyso adsorption/desorption with excellent desorption efficiency for three to four successive cycles, revealing the stability of coatings. Present work thus provides us with a new clue in the identification of key factors that can be utilized to design stimuli-responsive coatings which hold prospective for biomedical applications demanding the control of protein adsorption.

REFERENCES

1 Roach, P.; Farrar, D.; Perry, C. C. Surface tailoring for controlled protein adsorption: Effect of topography at the nanometer scale and chemistry. J. Am. Chem. Soc. 2006, 128(12), 3939−3945.

2 Lei, Z.; Gao, J.; Liu, X.; Liu, D.; Wang, Z. Poly(glycidyl methacrylate-*co*-2-hydroxyethyl methacrylate) brushes as peptide/protein microarray substrate for improving protein binding and functionality. ACS Appl. Mater. Interfaces 2016, 8(16), 10174−10182.

3 Chen, H.; Yang, J.; Xiao, S.; Hu, R.; Bhaway, M. S.; Vogt, D. B.; Zhang, M.; Chen, Q.; Ma, J.; Chang, Y.; Li, L.; Zheng, J. Salt-responsive polyzwitterionic materials for surface regeneration between switchable fouling and antifouling properties. Acta Biomater. 2016, 40, 62−69.

4 Liu, W.; Zhang, Y.; Fang, L.; Zhu, B.; Zhu, L. Antifouling properties of poly(vinly chloride) membranes modified by amphiphilic copolymers P(MMA-*b*-MAA). Chinese J. Polym. Sci. 2012, 30(4), 568−577.

5 Bettahalli, S. M. N.; Arkesteijn, M. T. I.; Wessling, M.; Poot, A. A.; Stamatialis, D. Corrugated round fibers to improve cell adhesion and proliferation in tissue engineering scaffolds. Acta Biomater. 2013, 9(6), 6928−6935.

6 Jana, S.; Tefft, J. B.; Spoon, B. D.; Simari, D. R. Scaffolds for tissue engineering of cardiac valves. Acta Biomater. 2014, 10, 2877−2893.

7 Tan, L.; Xing, J.; Cao, F.; Chen, L.; Zhang, C.; Shi, R.; Wang, Y. Synthesis of double-hydrophillic double-grafted copolymers PMA-*g*-PEG/PDMA and their protein-resistant properties. Chinese J. Polym. Sci. 2013, 31(4), 691−701.

8 Cavallaro, A. A.; MacGregor-Ramiasa, N. M.; Vasilev, K. Antibiofouling properties of plasma-deposited oxazoline-based thin films. ACS Appl. Mater. Interfaces 2016, 8(10), 6354−6362.

9 Demirci, S.; Kinali-Demirci, S.; Jiang, S. A switchable polymer brush system for antifouling and controlled detection. Chem. Commun. 2017, 53(26), 3713−3716.

10 Gao, F.; Xing, Y.; Yao, Y.; Sun, L.; Sun, Y.; He, X.; Lin, S. Self-assembly and multi-stimuli responsive behavior of PAA-*b*-PAzoMA-*b*-PNIPAM triblock copolymers. Polym. Chem. 2017, 8(48), 7529−7536.

11 Alas, R. G.; Agarwal, R.; Collard, M. D.; García, J. A. Peptide-functionalized poly[oligo(ethylene glycol) methacrylate] brushes on dopamine-coated stainless steel for controlled cell ddhesion. Acta Biomater. 2017, 59, 108−116.

12 Hoy, O. B.; Zdyrko, B.; Lupitskyy, R.; Sheparovych, R.; Aulich, D.; Wang, J.; Bittrich, E.; Eichhorn, K.; Stamm, M.; Uhlmann, P.; Hinrichs, K.; Mu, M.; Minko, S.; Luzinov, I. Synthetic hydrophilic materials with tunable strength and a range of hydrophobic interactions. Adv. Funct. Mater. 2010, 20(14), 2240−2247.

13 Delcroix, F. M.; Huet, L. G.; Conard, T.; Du Prez, E. F.; Landoulsi, J. Design of mixed PEO/PAA brushes with switchable properties toward protein adsorption. Biomacromolecules 2012, 14(1), 215−225.

14 Delcroix, F. M.; Huet, L. G.; Conard, T.; Demoustier-Champagne, S.; Du Prez, E. F.; Landoulsi, J.; Dupont-Gillain, C. C. Quartz crystal microbalance study of ionic strength and pH dependent polymer conformation and protein adsorption/desorption on PAA, PEO, and mixed PEO/PAA brushes. Langmuir 2013, 30(1), 268−277.

15 Delcroix, F. M.; Laurent, S.; Huet, L. G.; Dupont-Gillain, C. C. Protein adsorption can be reversibly switched on and off on mixed PEO/PAA brushes. Acta Biomater. 2015, 11, 68−79.

16 Bratek-skicki, A.; Eloy, P.; Morga, M.; Dupont-gillain, C. Reversible protein adsorption on mixed PEO/PAA polymer brushes: Role of ionic strength and PEO content. Langmuir 2018, 34(9), 3037−3048.

17 Mero, A.; Pasut, G.; Dalla, L.; Fijten, M. W. M.; Schubert, S. U.; Hoogenboom, R.; Veronese, M. F.. Synthesis and characterization of poly(2-ethyl-2-oxazoline)-conjugates with proteins and drugs: Suitable alternatives to PEG-conjugates. J. Control. Release 2008, 125(2), 87−95.

18 Chen, Y.; Pidhatika, B.; Erlach, V. T.; Konradi, R.; Textor, M.;

Hall, H. Comparative assessment of the stability of nonfouling poly(2-methyl-2-oxazoline) and poly(ethylene glycol) surface films: An *in vitro* cell culture study. Biointerphases 2014, 9(3), 031003.

19 Tan, L.; Bai, L.; Zhu, H.; Zhang, C.; Chen, L.; Wang, Y.; Cheradame, H. Stable antifouling coatings by hydrogen-bonding interaction and poly(acrylic acid). J. Mater. Sci. 2015, 50(14), 4898−4913.

20 Zhu, H.; Mumtaz, F.; Zhang, C.; Tan, L.; Liu, S.; Zhang, Y.; Pan, C.; Wang, Y. A rapid approach to prepare poly(2-methyl-2-oxazoline)-based antifouling coating by UV irradiation. Appl. Surf. Sci. 2017, 426, 817−826.

21 Pan, C.; Liu, X.; Gong, K.; Mumtaz, F.; Wang, Y. Dopamine assisted PMOXA/PAA brushes for their switchable protein adsorption/desorption. J. Mater. Chem. B 2018, 6, 56−567.

22 Mumtaz, F.; Chen, C.; Zhu, H.; Pan, C.; Wang, Y. Controlled protein adsorption on PMOXA/PAA based coatings by thermally induced immobilization. Appl. Surf. Sci. 2018, 439, 148−159.

23 Du, J.; Willcock, H.; Patterson, P. J.; Portman, I.; O'Reilly, K. R. Self-assembly of hydrophilic homopolymers: a matter of RAFT end groups. Small 2011, 7(14), 2070−2080.

24 Zeinali, E.; Haddadi-Asl, V.; Roghani-Mamaqani, H. Nanocrystalline cellulose grafted random copolymers of *N*-isopropylacrylamide and acrylic acid synthesized by RAFT polymerization: effect of different acrylic acid contents on LCST behavior. RSC Adv. 2014, 4(59), 31428−31442.

25 Qu, Z.; Hu, F.; Chen, K.; Duan, Z.; Gu, H.; Xu, H. A facile route to the synthesis of spherical poly(acrylic acid) brushes *via* RAFT polymerization for high-capacity protein immobilization. J. Colloid Interface Sci. 2013, 398, 82−87.

26 Bai, L.; Tan, L.; Chen, L.; Liu, S.; Wang, Y. Preparation and characterizations of poly(2-methyl-2-oxazoline) based antifouling coating by thermally induced immobilization. J. Mater. Chem. B 2014, 2(44), 7785−7794.

27 Liu, G.; Zhang, G. Collapse and swelling of thermally sensitive poly(*N*-isopropylacrylamide) brushes monitored with a quartz crystal microbalance. J. Phy. Chem. B 2005, 109(2), 743−747.

28 Dong, R.; Lindau, M.; Ober, K. C. Dissociation behavior of weak polyelectrolyte brushes on a planar surface. Langmuir 2009, 25(8), 4774−4779.

29 Aulich, D.; Hoy, O.; Luzinov, I.; Brücher, M.; Hergenröder, R.; Bittrich, E.; Eichhorn, J. K.; Uhlmann, P.; Stamm, M.; Esser, N.; Hinrichs, K. *In situ* studies on the switching behavior of ultrathin poly(acrylic acid) polyelectrolyte brushes in different aqueous environments. Langmuir 2010, 26(15), 12926−12932.

30 Yadav, V.; Harkin, V. A.; Robertson, L. M.; Conrad, C. J. Hysteretic memory in pH-response of water contact angle on poly(acrylic acid) brushes. Soft Matter 2016, 12(15), 3589−3599.

31 Belegrinou, S.; Mannelli, I.; Lisboa, P.; Bretagnol, F.; Valsesia, A.; Ceccone, G.; Colpo, P.; Rauscher, H. pH-Dependent immobilization of proteins on surfaces functionalized by plasma-enhanced chemical vapor deposition of poly(acrylic acid) and poly(ethylene oxide) like films. Langmuir 2008, 24(11), 7251−7261.

32 Wang, W.; Cui, M.; Song, Z.; Luo, X. An antifouling electrochemical immunosensor for carcinoembryonic antigen based on hyaluronic acid doped conducting polymer PEDOT. RSC Adv. 2016, 6(91), 88411−88416.

33 Luo, L Y..; Zhang, Y. X.; Wang, Y.; Han, J. F.; Xu, F.; Chen, S. Y. Mediating physicochemical properties and paclitaxel release of pH-responsive H-type multiblock copolymer self-assembly nanomicelles through epoxidation. J. Mater. Chem. B 2017, 5(17), 3111−3121.

34 Christener, M. N. A. J.; Honeyman, D. B. Influence of aqueous pH and ionic strength on the wettability of quartz in the presence of dense non-aqueous-phase liquids. Environ. Sci. Technol. 1997, 31(3), 676−681.

35 Konradi, R.; Pidhatika, B.; Mühlebach, A.; Textor, M. Poly-2-methyl-2-oxazoline: A peptide-like polymer for protein-repellent surfaces. Langmuir 2008, 24(3), 613−616.

36 Pidhatika, B.; Möller, J.; Vogel, V. ; Konradi, R. Nonfouling surface coatings based on poly(2-methyl-2-oxazoline). CHIMIA. Int. J. Chem. 2008, 62(4), 264−269.

37 Dai, J.; Bao, Z.; Sun, L.; Hong, U. S.; Baker, L. G.; Bruening, L.M. High-capacity binding of proteins by poly(acrylic acid) brushes and their derivatives. Langmuir 2006, 22(9), 4274−4281.

38 Swift, T.; Swanson, L.; Geoghegan, M.; Rimmer, S. The pH-responsive behaviour of poly(acrylic acid) in aqueous solution is dependent on molar mass. Soft Matter 2016, 12(9), 2542−2549.